International Journal of Multiphase Flow 83 (2016) 232–238

Contents lists available at ScienceDirect

International Journal of Multiphase Flow

journal homepage: www.elsevier.com/locate/ijmultiphaseflow

Thrust generation by pulse combustion of gas in a submerged chamber

R.N. Medvedev*, A.P. Drozhzhin, V.S. Teslenko

Lavrent'ev Institute of Hydrodynamics, Siberian Branch, Russian Academy of Sciences, Lavrent'ev avenue 15, Novosibirsk, 630090 Russia

ARTICLE INFO

Article history:
Received 3 August 2015
Revised 4 February 2016
Accepted 6 April 2016
Available online 13 April 2016

Keywords:
Underwater combustion
Bubble pulsation
Propulsion device
Hydro-jet engine

ABSTRACT

This paper presents the results of experimental and theoretical studies of the hydrodynamic processes occurring during gas combustion in a vertical cylindrical chamber submerged in water. It is shown that combustion of a single portion of a stoichiometric propane–oxygen mixture leads to cyclic generation of force impulses on the thrust wall: the first impulse is generated due to the combustion of gas, and the subsequent impulses are generated due to hydrodynamic oscillations of the gas cavity. A total specific impulse of 10^4–10^5 s (10^5–10^6 m/s) was experimentally obtained.

Expressions for the adiabatic oscillation period of the gas cavity and the maximum impulse of the force acting on the thrust wall during expansion of the cavity were obtained by approximate calculations. It is shown that the period is proportional to the length of the chamber to a power of 0.65, and the maximal force impulse is proportional to the square root of the length of the chamber. The oscillation periods calculated from the maximum size of the cavity are in good agreement with experimentally measured period of the first pulsation. Calculated force impulses are larger than experimental ones, which is attributed to thermal and hydrodynamic losses.

The results of the study are applicable to water propellers, devices for regenerating filters, generating acoustic waves, and cleaning underwater bodies.

1. Introduction

At present, waterborne vehicles use petrol and diesel internal combustion engines (ICEs) with screw propellers. The main disadvantages of such propulsion systems are large losses due to friction in the chain of transfer of mechanical energy from the combustion chamber to the propeller screw. ICEs are complicated in construction and have high manufacturing and maintenance costs and the use of natural gas as fuel reduces the engine life. Therefore, the search for ways to reduce mechanical energy losses in ship propulsion plants still remains relevant. One such way is to use the combustion products to eject the water mass from the chamber submerged in water and attached to the ship hull.

Pulse combustion of fuel directly in water on the thrust wall for thrust generation has been studied previously (Teslenko et al., 2014, Teslenko et al., 2014). The developed principle is similar to the principle of operation of the Humphrey pump, which was invented at the beginning of the last century and offered a significant benefit over other types of pumps for pumping large volumes of water (The Humphrey internal combustion pump, 1913, McLauchlan, 1931). Later, various researchers have used similar principles to develop propulsion systems based on thrust generation by ejection of a water column by fuel combustion products (Saurer and Victora, 1952, Kaminstein, 1964, Colautti, 2009). These types of propulsion are called impulse hydro-jet engines. Fundamental features that distinguish these engines from classical internal combustion engines are, first, the absence of structural components moving relative to each other and, hence, the absence of friction between them, which is an advantage. Second, combustion occurs in water vapor. It is known, however, that water vapor is a combustion inhibitor reducing the pressure in the cavity (Gelfand et al., 2012), which adversely affects the efficiency. The absence of screw removes the additional restrictions on the thrust associated with cavitation. Furthermore, by optimizing the design, it is possible to make the best use of the potential energy of the burned gas to perform work, whereas in internal combustion engines, it is limited by the maximum piston stroke. Thus, the question of the superiority of the total efficiency of impulse hydro-jet engines remains open.

The fundamental principles of impulse hydro-jet engines have been developed in studies of underwater explosions. For example, an underwater explosion of gas mixtures has been investigated

* Corresponding author. Tel.: +73833333047; fax: +73833333047.
E-mail address: ruslan@hydro.nsc.ru (R.N. Medvedev).

http://dx.doi.org/10.1016/j.ijmultiphaseflow.2016.04.001
0301-9322/

(Popov and Kogarko, 1976, Ivashechkin and Veremenuk, 2009, Kogarko et al., 1975) for the purposes of regenerating well screens and marine geology applications. The studies cited considered combustion in a spherical bubble filled with fuel gas and in a semi-enclosed cylinder, fully or partially filled with gas. Approximation relations for the maximum size of the cavity and the force impulse generated during bubble growth have been derived (Ivashechkin and Veremenuk, 2009). These relations were obtained for use in the design of facilities for reworking a well and are applicable in a narrow range of geometric parameters.

The processes occurring during underwater explosion of solid explosives have been extensively studied since the beginning of the last century. A large number of papers have been devoted to experimental studies of shock waves and hydrodynamic flows and mathematical models that take into account compressibility, viscosity, and surface tension (Rayleigh, 1917, Lauterborn and Kurz, 2010, Shah et al., 1999, Franc and Michel, 2005, Kedrinskiy, 2005). In almost all the papers, a spherical bubble shape is considered, as the most common in underwater explosion and cavitation, and bubble oscillations are studied in an infinite or semi-infinite space. In the calculations, adiabatic approximations are mainly used, the energy release is assumed to be instantaneous, and the gas pressure inside the bubble is neglected almost throughout the period of oscillation. These approximations are suitable for describing the oscillations of the detonation products of solid explosives under water, which is confirmed by the good agreement between theory and the results of experiments.

In the theoretical description of the combustion of fuel gas in water, assumptions suitable for describing underwater explosion may be incorrect due to much lower burning rates and energy release density (Popov and Kogarko, 1976). It becomes necessary to consider the time of the chemical reaction and heat transfer during oscillations of the combustion products. On the other hand, acoustic losses are reduced to a few percent (Kogarko et al., 1975), making it possible to neglect the compressibility of the liquid. The range of possible applications of underwater gas explosions (regeneration of the filter, thrust generation) involves the use of limited volumes (pipes, nozzles), which significantly complicates the nature of hydrodynamic flows, requiring consideration of edge defects (Teslenko et al., 2014, Morteza et al., 1998, Kruegera and Gharib, 2003, Koita et al., 2012).

For spherical gas explosions (Teslenko et al., 2010), the maximum cavity size is comparable to the value calculated in the adiabatic approximation (Popov and Kogarko, 1976), whereas for explosions in a cylindrical chamber, the maximum volume of the cavity is considerably smaller, which makes it impossible to carry out accurate calculations neglecting heat and mass exchange. Nevertheless, assuming that the ratio of the heat losses to the initial energy of the combustion products is the same, it is possible to obtain approximate estimates. The presence of essential heat losses leads to the fact that at the moment of collapse the pressure in cavity may exceed the initial pressure during the combustion of gas that is observed in (Teslenko et al., 2014, Teslenko et al., 2014, Popov and Kogarko, 1976) and in this work.

It has been shown (Teslenko et al., 2014) that combustion of a bubble near a rigid wall produces a thrust directed along the normal to the surface of the wall. The experimentally obtained specific impulse imparted to the thrust wall in one cycle of bubble combustion (impulse referred to the fuel mass) was $\approx 5{\cdot}10^4$ s ($5{\cdot}10^5$ m/s), which is comparable with the performance of modern screw and hydro-jet propulsion systems. In the study cited, the bubble had the shape of a torus and was located on the surface of a horizontal wall.

The main performance parameters of pulsing hydro-jet propellers are thrust and specific impulse.

The average thrust is given by the relation

$$\langle F\rangle = \frac{1}{T}\int_0^T F dt, \tag{1}$$

where F is the total force exerted on the thrust wall along the axis of movement, T is the length of one combustion cycle, which is assumed to be equal to the period of oscillation of the cavity with the combustion products.

The specific impulse is defined as

$$I_{sp} = \frac{1}{m}\int_0^T F dt, \tag{2}$$

where m is the mass of fuel gas burned in one cycle. Usually, in engine calculations, thrust is in kilograms and specific impulse in seconds.

From (1), it is seen that to increase the thrust, it is necessary to increase the force generated by the combustion products (which is determined by the pressure in the combustion chamber and the area of the end part of the chamber) and to reduce the length of the combustion cycle, which is limited by the time of growth of the gas cavity containing the combustion products. The faster the acceleration of the attached liquid mass, the greater the propulsion thrust.

One way to increase the specific impulse is to restrict the liquid motion from the thrust wall in the lateral direction. Since the calculations show that the cylindrical form of the nozzle is optimal for thrust generation (Zhdan et al., 1994), in this work it is the cylindrical nozzle that is chosen for theoretical calculation of adiabatic cavity pulsations and estimates of specific and average thrust. In contrast to earlier similar calculations (Zhdan et al., 1994, Back et al., 1983) carried out for gaseous environment, in the present work the environment is an incompressible liquid. This changes the character of processes. In particular, in this case there is a clear combustible gas-liquid interface and the density of environment is constant. Nevertheless, experiments (Teslenko et al., 2014, Teslenko et al., 2014) showed that there are some qualitative similarities. For example, the dependence of thrust force on time has an alternating pulsating character, but the specific impulse increases with the nozzle length. The comparison of data (Zhdan et al., 1994) and (Teslenko et al., 2014) demonstrates that in liquid the achievable specific impulse is larger than that in gaseous atmosphere and it has the level of modern water propellers.

In the setup with liquid environment the calculation of cavity pulsation in a cylindrical tube and the estimates of specific and average thrust are carried out for the first time. The experimental part of the work allows us to estimate the accuracy of calculations performed.

Thus, the aim of this work is an experimental and theoretical study of physical processes occurring during combustion of a portion of gas in a cylindrical chamber placed in water. The results may be used to solve the problems of underwater acoustics, underwater thrust generation, forming the impulse high-velocity jets and cleaning underwater objects.

2. Experimental

Fig. 1 shows a principal diagram of the experiments. Plastic cylindrical chamber 2 was placed vertically in plexiglas cuvette 1 0.5 m high and filled with water. The chamber was filled with a combustible mixture 3 in the upper closed part connected to a pin-joint device 4. The combustible mixture was ignited by a spark of high-voltage power supply 5. Combustion of predetermined portions of the gas mixture in the chamber 2 led to ejection of the water column from the chamber, which provided generation of force impulses in the vertical direction. Force impulses

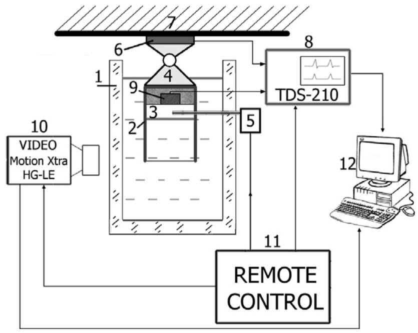

Fig. 1. Schematic diagram of the experimental setup.

were measured by a piezoelectric dynamometer 6, which was located between the pin-joint device 4 and a horizontal rigid beam 7. The piezo-dynamometer, 40 mm in diameter and 15 mm high, was made of lead zirconate–titanate (PZT) piezoceramics. The minimal time resolution of the piezoelectric dynamometer was 3 μs (the period of natural acoustic oscillations). Electrical signal from the piezoelectric dynamometer was sent to an emitter-follower amplifier with a time constant of 10 s and it was recorded using a Tektronix TDS-210 digital oscilloscope 8. To control the pressure inside the gaseous cavity 3, pressure pulses were measured using a tourmaline pressure transducer 9 with a period of natural acoustic oscillations of 0.3 μs. The pressure transducer was built in flush with the end of the chamber 2. Electrical signal from pressure transducer 9 was also sent to oscilloscope 8. The piezoelectric dynamometer and pressure transducers were calibrated before and after the experiments. The errors of the measured parameters were within 5–15%.

Shadowgraphs of hydrodynamic processes were taken with a MotionXtra HG-LE digital camera 10. The velocity of lower boundary motion of gaseous cavity 3 was determined with the use of filming.

The start of measurement systems and ignition spark was carried out by using a remote control 11. The measurement results were sent to a computer 12.

The experiments were performed with gaseous charges of a stoichiometric propane–oxygen mixture ($C_3H_8+5{\cdot}O_2$) of volume $V_0=3$ – 4 ml, which completely overlaps the cross section of the chamber. The inner diameter d of the chamber was 29 mm, and the height h was varied from 82 to 170 mm.

3. Experimental results

Fig. 2 shows recorded oscillograms of the force impulses $F(t)$ and overpressure pulses $P(t)$-P_a obtained simultaneously during combustion of 3 ml of a stoichiometric propane–oxygen mixture in a chamber 83 mm high (P_a is an atmospheric pressure).

Fig. 3 shows a shadowgraph of the hydrodynamic processes occurring during gas combustion in the cylindrical chamber ($V_0=3$ ml, $h=83$ mm). It is seen that almost over the whole cross-section except for a small part near the wall, the bubble boundary has a plane shape during the whole period of its growth. During the cavity collapse a jet formation can be seen in the central part (see Fig. 3, frame 6, $t=10.9$ ms).

In the third frame ($t=1.4$ ms), one can see a process of formation of a cavitating vortex ring on the bottom edge of the chamber (Teslenko et al., 2014), which then separates and propagates separately in the direction of liquid flow. The velocity of gaseous cavity expansion, at which cavitation begins to develop at the edge of the chamber, is in the range 2–3 m/s. In the same frame one can see a group of bubbles inside the chamber. This allows us to assume a formation of deformation wave moving along the chamber wall and causing cavitation processes on it.

The filming and measurements of the pressure pulses show that several force impulses were generated on the thrust wall during combustion of the single portion of the gas mixture (Fig. 2). The first impulse is generated owing to gas combustion and the subsequent impulses are generated due to collapse of the cavity containing combustion products and water vapor. Here several pulsations of the cavity are observed.

Processing of the force impulses and calculations of the specific impulses for this series of experiments show that, given the parameters used and measured, the total specific impulse is in the range $I_{sp}=10^4$–10^5 s (10^5–10^6 m/s). The range of the specific impulse depends on the choice of the ratio of height of the gaseous charge and the height of the chamber (see Fig. 6).

In the experimental studies of combustion of 3 ml of a stoichiometric propane–oxygen mixture in a chamber 83 mm high, the maximum pressure amplitudes ranged from 12 to 17 atm. These values are lower than those given in (Popov and Kogarko, 1976) for explosion of a spherical gaseous charge with a volume of 100 ml, which can be explained by the effect of water vapor and the insufficient size for the development of detonation.

Taking into account the fact that using a cylindrical chamber, the area of the thrust wall $S=$const, the thrust can be calculated by multiplying the cross-sectional area of the chamber by the gas pressure measured by the pressure transducer in the combustion chamber. The experiments showed that the values of thrust force calculated by the results of pressure measurement $F_p(t)=(P(t)\text{-}P_a)\bullet S$ exceeded the force values measured directly by the dynamometer F_d. The values of $(F_p - F_d)/F_p$ ranged within 0.15–0.3. This indicates the presence of losses in the system which may be due to hydrodynamic processes (including cavitation).

4. Numerical simulation

To determine the relations between the thrust characteristics and the parameters of the system, we carried out a calculation of the problem in the formulation shown in Fig. 4. Thick lines represent a cylindrical chamber with a closed end which was the thrust wall. R and h are the radius and height of the tube, respectively, ($R=d/2$), and x is the height of the cylindrical gaseous cavity. The thickness of the chamber was assumed to be negligibly small compared to the radius. The liquid was considered ideal and incompressible. Based on the data of (Schlichting and Gersten, 2000), turbulence does not develop during the growth of the cavity (~10 ms) and at a chamber length of ~10 cm, so that the flow in the chamber can be assumed to be approximately potential.

The velocity field in the liquid υ was found by numerical simulation. For this, the Laplace equation $\frac{1}{\tilde r}\frac{\partial}{\partial \tilde r}(\tilde r\frac{\partial\tilde\varphi}{\partial\tilde r})+\frac{\partial^2\tilde\varphi}{\partial\tilde z^2}=0$ was numerically solved for the velocity potential $\tilde\varphi=\frac{\varphi}{R\dot x}$ in cylindrical coordinates with axial symmetry about the z axis (r is the distance from the z axis) using a finite element method on a nonuniform triangular grid. The grid size was $\tilde r\in(0:1000)$, $\tilde z\in(-1000:1000)$, where $\tilde r=r/R$, $\tilde z=z/R$.

In the calculation, zero velocity $\varphi|_{r,\,z\,\to\,\infty}\to 0$ was specified on the boundary of the integration region, zero normal velocity component $\frac{\partial\varphi}{\partial r}|_{r=0}=0$, $\frac{\partial\varphi}{\partial r}|_{r=R,z<h}=0$ was specified on the surface of the chamber wall and on the z axis, and the nonpenetration condition $\frac{\partial\varphi}{\partial z}|_{z=x,r\le R}=\dot x$ was imposed on the boundary of the bubble. The thickness of the chamber walls was assumed to be negligibly small compared to its radius.

Next, the kinetic energy of the liquid inside the chamber and in the whole volume was determined by the formula $\tilde K=\frac{K}{\rho\dot x^2R^3}=\frac{\pi}{3}\sum_i(\tilde\upsilon_{i,1}^2\tilde r_{i,1}+\tilde\upsilon_{i,2}^2\tilde r_{i,2}+\tilde\upsilon_{i,3}^2\tilde r_{i,3})S_i$, where S_i is the area of the i-th triangular element of the grid, the summation over the

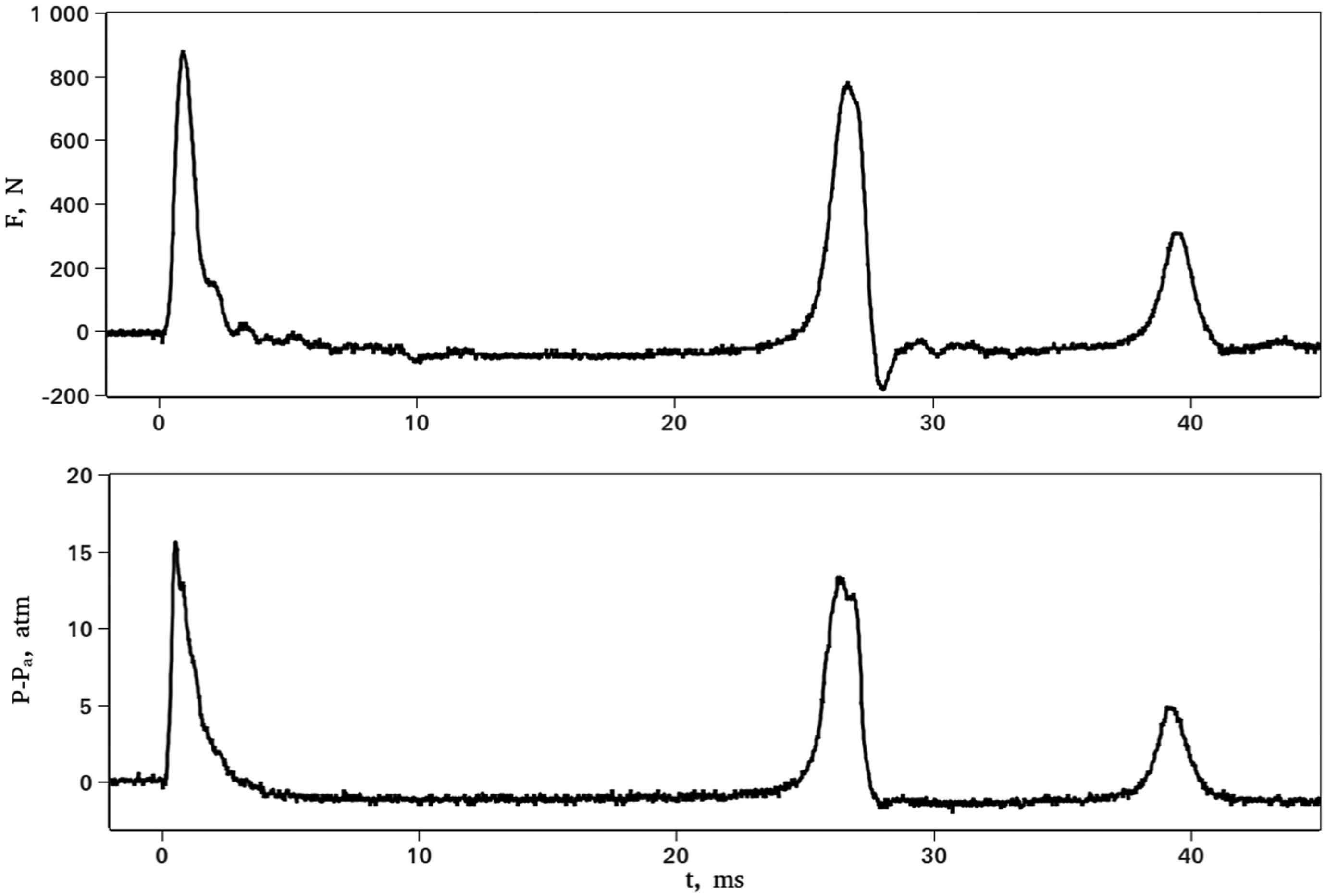

Fig. 2. Synchronously recorded oscillograms of force impulses F (t) and pressure pulses P(t)-P_a.

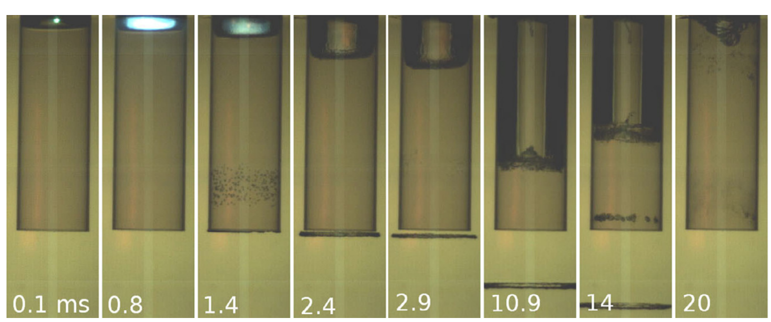

Fig. 3. Shadowgraph of the dynamics of the processes inside and outside the chamber for a gaseous charge with $V_0 = 3$ ml, d = 29 mm, and h = 83 mm..

nodes of each i-th triangular element of the grid is written in parentheses, $\tilde{\upsilon} = \upsilon/\dot{x}$, ρ is the density of the liquid.

The results show that under the assumption of a long chamber ($h \gg x$), most of the kinetic energy belongs to the liquid column inside the chamber. For example, at a ratio $x/h = 0.4$, 90% of the kinetic energy is concentrated in the chamber, and at $x/h = 0.8$, 74%. Thus, for approximate calculations, the liquid flow outside the chamber can be neglected.

The kinetic energy of the flow ejected from the chamber is expended in the formation and motion of the vortex ring because the jet leaving the chamber does not spread completely but forms a vortex ring, which can make an additional contribution to the kinetic energy and hence the thrust. The effect of the vortex on the thrust was studied in (Kruegera and Gharib, 2003), where for a chamber length to diameter ratio $h/d = 3$, a contribution of 30% was obtained. In addition, it is said in the paper that the vortex affects the thrust until its separation from the edge of the chamber since the formation of the vortex is accompanied by deceleration of the flow and generation of excess pressure at the chamber outlet. In our case, vortex separation occurs at the initial stage of expansion of the cavity (Fig. 3, 2.4 ms), so that in these approximate calculations, its influence is ignored, but in future studies, it should be given special attention.

In view of the above assumptions, the law of conservation of energy is written as

$$E = K + A + U = const \quad (3)$$

where K is the kinetic energy of the liquid (in our approximation, $K \approx \frac{\rho S \dot{x}^2 (h-x)}{2}$), $A = P_a \cdot S(x - x_0)$ is the work done against the external pressure forces, U is the internal energy of the cavity (in the case of an ideal gas, $U = \frac{PSx}{\gamma - 1}$). Here x_0 is the initial size of the cavity, P and P_0 are the pressure and initial pressure inside the

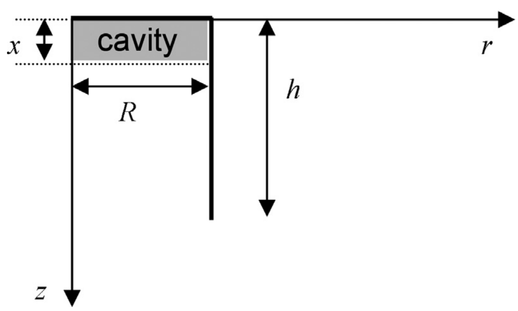

Fig. 4. Mathematical formulation of the problem of cavity pulsation in a cylindrical chamber.

cavity, P_a is the pressure in the surrounding liquid ($P_0 > P_a$), ρ is the density of the liquid, $S = \pi R^2$ is the cross-sectional area of the chamber, γ is the adiabatic index of the gas in the bubble (≈ 1.24 for propane–oxygen mixtures (Popov and Kogarko, 1976)).

In contrast to solid explosions, for the underwater gas explosion in the chamber, the energy carried away by the shock wave is fractions of a percent (Kogarko et al., 1975) and hence can be neglected in the estimation.

We assume that at the boundary of the cavity, there is no heat and mass transfer. Then the pressure in the cavity is given by the expression

$$P = P_0 (x_0/x)^{\gamma} \tag{4}$$

At the initial time, K and A are zero, so that $E = \frac{P_0 S x_0}{\gamma - 1}$. Substituting this expression into (3), expressing the pressure by formula (4), and reducing the cross-sectional area of the chamber S, we obtain the relation

$$\frac{P_0 x_0}{\gamma - 1} = \frac{\rho (h - x) \dot{x}^2}{2} + (x - x_0) P_a + \frac{P_0 x}{\gamma - 1} \left(\frac{x_0}{x} \right)^{\gamma} \tag{5}$$

(it is assumed that γ does not change appreciably during the expansion of the cavity). Expressing the cavity growth rate from relation (5), we obtain

$$\dot{x} = \frac{dx}{dt} = \sqrt{\frac{2}{\rho (h - x)} \left(\frac{P_0 x_0}{\gamma - 1} - \frac{P_0}{\gamma - 1} \frac{x_0^{\gamma}}{x^{\gamma - 1}} - (x - x_0) P_a \right)}. \tag{6}$$

From this expression, we can find the period of cavity pulsation by bringing dt to the right side, and integrating:

$$T = \sqrt{2\rho} \int_{x_0}^{x_{\max}} \frac{\sqrt{h - x}}{\sqrt{\frac{P_0 x_0}{\gamma - 1} - \frac{P_0}{\gamma - 1} \frac{x_0^{\gamma}}{x^{\gamma - 1}} - (x - x_0) P_a}} dx, \tag{7}$$

where $x_{\max}$ is the maximum size of the cavity ($x_{\max} < h$). Formula (7) is conveniently represented in dimensionless form

$$\tilde{T} = \int_1^{\tilde{x}_{\max}} \sqrt{\frac{\tilde{h} - \tilde{x}}{\frac{\tilde{P}_0}{(\gamma - 1)} \left(1 - \tilde{x}^{1 - \gamma} \right) - \tilde{x} + 1}} d\tilde{x}, \tag{8}$$

where $\tilde{T} = T \frac{1}{x_0} \sqrt{\frac{2 P_a}{\rho}}$, $\tilde{P}_0 = P_0 / P_a$, $\tilde{x} = x / x_0$, $\tilde{x}_{\max} = x_{\max} / x_0$, $\tilde{h} = h / x_0$.

The integral in (8) is not found analytically. The results of the numerical integration for $\gamma = 1.24$ can be approximated by the relation

$$\tilde{T} \approx 4.2 \left(\tilde{h} - \tilde{x}_{\max} \right)^{0.65} + 1.15 (\tilde{x}_{\max} + 2.7). \tag{9}$$

At the end of the expansion of the cavity at maximum size ($x = x_{\max}$), the kinetic energy is zero. Writing the equality of the energy E at zero time ($x = x_0$) and that at the time when the cavity has a maximum size ($x = x_{\max}$) and using expression (4), we obtain the following relation between P_0 and $x_{\max}$:

$$\frac{P_0 x_{\max}}{\gamma - 1} \left(\frac{x_0}{x_{\max}} - \frac{x_0^{\gamma}}{x_{\max}^{\gamma}} \right) = P_a (x_{\max} - x_0). \tag{10}$$

From this, knowing the maximum size of the cavity, we can calculate the initial pressure in it. In dimensionless form, it is defined as

$$\tilde{P}_0 = (\gamma - 1) \frac{\tilde{x}_{\max} - 1}{1 - \tilde{x}_{\max}^{1 - \gamma}}. \tag{11}$$

We estimate the ***impulse of the force I*** exerted on the thrust wall by the cavity. It is equal to $I = S \int (P - P_a) dt$. It is evident that the integral has a maximum at the time when $P = P_a$. At this time, $x = x_a = x_0 \left(\frac{P_0}{P_a} \right)^{1/\gamma}$. Expressing dt by formula (6) and the pressure from (4) and using x_a, as the upper limit of integration, we express the maximum impulse as

$$I_{\max} = V_0 \sqrt{\frac{P_a \rho}{2}} \int_1^{\tilde{x}_a} \left(\tilde{P}_0 \tilde{x}^{-\gamma} - 1 \right) \sqrt{\frac{\tilde{h} - \tilde{x}}{\frac{\tilde{P}_0}{\gamma - 1} \left(1 - \tilde{x}^{1 - \gamma} \right) - \tilde{x} + 1}} d\tilde{x}, \tag{12}$$

where $V_0 = S x_0$ is the initial volume of the burnt gas.

Eq. (12) can be represented in dimensionless form as

$$\tilde{I}_{\max} = \frac{I_{\max}}{V_0 \sqrt{P_a \rho}} = \frac{1}{\sqrt{2}} \int_1^{\tilde{x}_a} \left(\tilde{P}_0 \tilde{x}^{-\gamma} - 1 \right) \sqrt{\frac{\tilde{h} - \tilde{x}}{\frac{\tilde{P}_0}{\gamma - 1} \left(1 - \tilde{x}^{1 - \gamma} \right) - \tilde{x} + 1}} d\tilde{x}. \tag{13}$$

The integral in (13) does not have an analytical primitive, and for $\gamma = 1.24$, it can be approximated by the relation $3.2 \sqrt{\tilde{h}} (\sqrt{\tilde{P}_0} - 1)$. Thus:

$$\tilde{I}_{\max} \approx 2.26 \sqrt{\tilde{h}} \left(\sqrt{\tilde{P}_0} - 1 \right). \tag{14}$$

Since for the same equivalence ratios of fuel and oxidant, the volume of the burnt gas V_0 is proportional to the fuel mass, the dimensionless impulse $\tilde{I}_{\max}$ has the meaning of the ***specific impulse*** I_{sp} to within a constant factor. To obtain maximum impulse in each cycle of combustion, it is necessary to provide a supply of the next portion of water into the combustion chamber when the pressure in the cavity is reduced to the pressure in the incoming flow.

Using formulas (9) and (14), we write the following approximate relation for the ***average thrust*** in the optimal mode of operation:

$$\langle F \rangle = \frac{I_{\max}}{T} = \frac{V_0 \sqrt{P_a \rho}}{x_0 \sqrt{2 \rho / P_a}} \frac{\tilde{I}_{\max}}{\tilde{T}}$$

$$\approx \frac{S P_a}{\sqrt{2}} \frac{\sqrt{\tilde{h}} \left(\sqrt{\tilde{P}_0} - 1 \right)}{1.86 \left(\tilde{h} - \tilde{x}_{\max} \right)^{0.65} + 0.5 (\tilde{x}_{\max} + 2.7)}. \tag{15}$$

It is seen that the average thrust is proportional to the cross-sectional area and, hence, to the gas volume V_0 with all other parameters fixed.

In dimensionless form, the average thrust is given by the expression

$$\langle \tilde{F} \rangle = \frac{\tilde{I}_{\max}}{\tilde{T}} \approx \frac{\sqrt{\tilde{h}} \left(\sqrt{\tilde{P}_0} - 1 \right)}{1.86 \left(\tilde{h} - \tilde{x}_{\max} \right)^{0.65} + 0.5 (\tilde{x}_{\max} + 2.7)}. \tag{16}$$

In the calculations, the energy loss due to water friction on the chamber walls during the growth of the cavity is neglected. We estimate these losses. The work to overcome friction is defined as $A_f = \Delta P (h - x_0) S$, where ΔP is the pressure loss between the cavity and the chamber outlet, which is determined from the expression $\Delta P = \lambda \frac{h - x}{d} \frac{\rho \dot{x}^2}{2}$ (Schlichting and Gersten, 2000). The friction coefficient λ for smooth tubes is found from the relation $\lambda^{-0.5} = 2 \lg (\mathrm{Re} \cdot \lambda^{0.5}) - 0.8$ (Schlichting and Gersten, 2000). In our case, $\dot{x} \le 10$ m/s, $h - x_0 \sim 10$ cm, $d = 30$ mm, $\mathrm{Re} = \frac{\dot{x} d}{\nu} \sim 10^5$ (ν is a

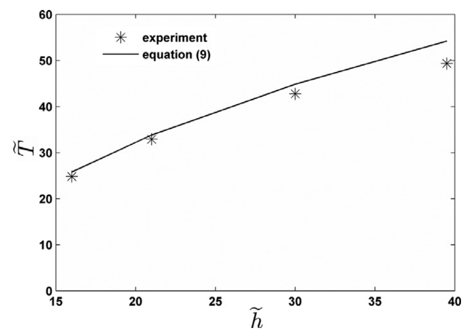

Fig. 5. Dependence of the experimental and calculated values of the first cavity oscillation period T on the chamber length h in dimensionless variables.

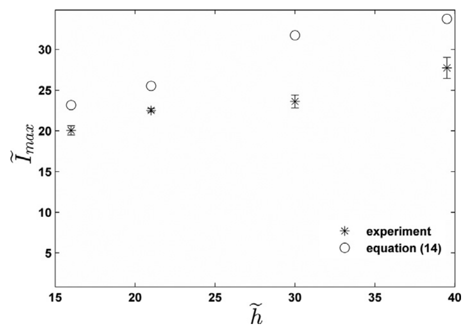

Fig. 6. Experimental and calculated values of the dimensionless impulse versus relative length of the chamber.

kinematic viscosity of water at temperature 25 °C), the friction coefficient $\lambda \approx 0.02$, and, hence, the pressure loss is $\Delta P \sim 0.03$ atm. The work to overcome friction $A_f \sim 0.2$ J. Based on the measured pressures, the internal energy of a cavity of volume 3 ml immediately after the combustion of the propane–oxygen mixture will be $\approx$ 15 J. It can be seen that for combusted gas volumes V_0 >1 ml, the losses due to friction can be neglected.

Unfortunately, the losses associated with the development of cavitation processes in the chamber are still difficult to evaluate.

5. Comparison of the simulation and experiment

Fig. 5 shows the experimental dependence of the dimensionless oscillation period of the first oscillation of the cavity in comparison with the result of calculation by formula (9). The experimental points were obtained by averaging over at least four experiments. In the calculation by formula (9), the maximum experimental sizes of the cavity $x_{\max}$ were used. It can be seen that for small $\tilde{h}$, the calculated values of the oscillation period are in good agreement with experimental measurements, and with an increase in $\tilde{h}$ (which corresponds to an increase in the length of the chamber or a decrease in the ejected gas volume), there is a discrepancy which is attributed to increased heat losses due to the longer time of growth and collapse of the cavity.

Fig. 6 shows the results of measurement of the first thrust impulse up to the moment of reduction of the thrust to zero in comparison with the results of calculation by formula (14). Each experimental point represents the results of at least four experiments; in formula (14), experimental initial pressure was used. It can be seen that the experimental values are lower than the calculated ones, and the difference increases with increasing *h*, which is also attributed to increased heat loss as the oscillation period increases. One can also see that $\tilde{I}_{\max}$ increases with increasing relative length of the chamber, i.e., the specific impulse I_{sp} will also increase. It is reasonable to assume that at a certain $\tilde{h}_{opt}$, the heat losses and

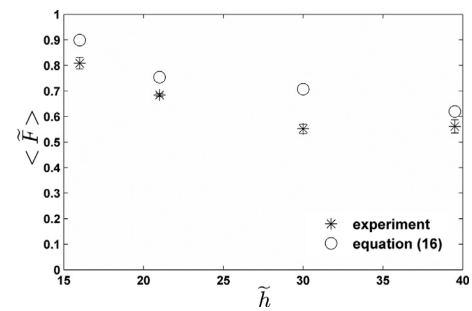

Fig. 7. Experimental and calculated values of the dimensionless average thrust versus relative length of the chamber.

friction become so large that the specific impulse ceases to grow. Therefore, to obtain maximum specific impulse, it is necessary that the length of the chamber be close to $\tilde{h}_{opt}$. This will be addressed in future work.

Fig. 7 shows the experimental and calculated (by formula (16)) dependences of the dimensionless average thrust on the length of the chambers. It is seen that the average thrust, in contrast to the specific impulse, increases with decreasing length of the chamber and reaches a maximum at $\tilde{h} = \tilde{x}_{\max}$. The same conclusion follows from the analysis of formula (16).

The maximum possible average thrust (at $\tilde{h} = \tilde{x}_{\max}$) can be expressed as

$$\langle F\rangle_{\max} \approx \sqrt{2}SP_a \frac{\sqrt{\tilde{x}_{\max}}\left(\sqrt{\tilde{P}_0}-1\right)}{\tilde{x}_{\max}+2.7}. \tag{17}$$

For propane–oxygen mixtures ($P_0 = 15$ atm, $\tilde{x}_{\max} \approx 20$) the maximum average thrust is $\langle F\rangle_{\max} \approx 0.8SP_a$.

The above calculation in adiabatic approximation assumes the identity of the first and all subsequent periods of cavity pulsations (if the hydrodynamic losses are ignored). However, as it can be seen from Fig. 2, the period of the second pulsation is approximately 2 times shorter than the first one (moreover, the ratio of the periods close to two is observed for all lengths of chambers and all volumes V_0 used in experiment). This demonstrates the essential losses in the process of the cavity pulsations. Another proof of water vapor condensation in gaseous cavity is the fact that the cavity size at the moment of collapse is less than the initial one at the moment of initiation (Fig. 3) (Kogarko et al., 1975). By using formula (9), it is possible to estimate which part of energy was expended for losses during the period of the cavity pulsation. Since the pressure in the first and second pulses is approximately same (Fig. 2), according to (10) the value $\tilde{x}_{\max}$in the first and second periods will be different slightly, but $\tilde{h}$ will increase in the second period as many times as internal energy of the cavity will decrease after the first pulsation $\frac{\tilde{h}_2}{\tilde{h}_1} = \frac{x_0}{x_1} = \frac{U_0}{U_1}$, where U_0 is the internal energy of the cavity at the initial moment of time, x_1 and U_1 is the size of cavity and its internal energy during collapse at the moment of time T_1. Writing the ratio of periods as $\frac{\tilde{T}_1}{\tilde{T}_2} = \frac{T_1}{T_2}\frac{x_1}{x_0} = \frac{T_1}{T_2}\frac{U_1}{U_0} \approx 2\frac{U_1}{U_0}$ and using formula (9), we can find the ratio $\frac{U_0}{U_1}$. For $\tilde{h}$= 30 – 40 the ratio $\frac{U_0}{U_1} \approx 6$.

From the graph in Fig. 6, it is possible to define in a similar way which part of energy is lost during the period of effective work operation. The analysis with the use of formula (14) shows that it is 15-30%. It is appeared that in experiment the pressure in the cavity decreases quicker than it does in calculation and so the integral and, hence, the impulse turn out to be less.

Thus, the losses during the combustion of gas mixtures in liquid are considerable that requires paying special attention to problems of heat and hydrodynamic losses during development of propulsion devices.

6. Conclusions

In the integrated experiments with simultaneous measurements of the thrust, pressure, and hydrodynamic processes inside and outside the chamber, a specific impulse up to 10^5 s (10^6 m/s) was obtained during combustion of a propane–oxygen mixture in a submerged chamber.

The results of the numerical simulation show that the kinetic energy of the liquid outside the chamber is a small part of the total kinetic energy and hence can be neglected in the estimation.

The initial pressure, oscillation period, specific impulse, and average thrust were calculated in the adiabatic approximation.

Comparison of the calculated and experimental results shows that at initial pressures in the bubble of 12–17 atm, the cavity volume increases by a factor of 17–23, which is 1.5–2 times less than the calculated values. This is obviously due to thermal and hydrodynamic losses. The losses are also responsible for the fact that experimental values of the specific impulse and average thrust are below the calculated values.

Analysis of the obtained dependences suggests that to achieve maximum specific impulse, the length of the chamber should be increased, and to achieve maximum average thrust, it should be decreased.

The results of this work can be used as a basis for the development of relatively simple pulsating hydro-jet propulsion systems based on hydrocarbon combustion directly in water on the thrust wall, as well as for the design of devices for filter regeneration, generation of acoustic waves, and cleaning underwater bodies.

Acknowledgments

This work was supported by RFBR grant Nos. 13-08-00838 and 14-08-00226.

We thank Dr. Sergey Zhdan for useful discussion of the work!

References

Back, LloydH., Dowler, WarrenL., Varsi, Giulio, 1983. Detonation Propulsion Experiments and Theory. AIAA J. 21 (10), 1418–1427. doi:10.2514/3.8262.

Colautti, E. Nautical engine for boats, Italy Patent WO2009/078049, June 25, 2009.

Franc, Jean-Pierre, Michel, Jean-Marie, 2005. Fundamentals of Cavitation. Springer, Netherlands doi:10.1007/1-4020-2233-6.

Gelfand, B.E., Silnikov, M.V., Medvedev, S.P., Khomik, S.V., 2012. Thermo-Gas Dynamics of Hydrogen Combustion and Explosion. Springer eBooks, Novosibirsk doi:10.1007/978-3-642-25352-2.

Ivashechkin, V.V., Veremenuk, V.V., 2009. Hydrodynamics of underwater gas explosion in half-closed chamber situated in well. In: ENERGETIKA. Proceedings of CIS Higher Education Institutions and Power Engineering Associations, pp. 74–81.

Kaminstein, B. Hydrojet propulsion apparatus, U.S. Patent 3137997, June 23, 1964.

Kedrinskiy, V., 2005. Hydrodynamics of Explosion. Springer-Verlag, Berlin Heidelberg.

Kogarko, S.M., Popov, O.E., Novikov, A.S., 1975. Underwater explosion of a gas mixture as a source of pressure waves. Combustion, explosion and shock waves 11 (5), 648–654. doi:10.1007/BF00751092.

Koita, T., Zhu, Y., Sun, M., 2012. Investigation of bubble collapse and water jet induced by underwater explosion in a rectangular tube. In: Proc. of the 28th International Symposium on Shock Waves, Vol. 2, pp. 27–32. doi:10.1007/978-3-642-25685-1_5.

Kruegera, PaulS., Gharib, M., 2003. The significance of vortex ring formation to the impulse and thrust of a starting jet. Phys. Fluids 15 (5), 1271–1281. doi:10.1063/1.1564600.

Lauterborn, W., Kurz, T., 2010. Physics of bubble oscillations. Rep. Prog. Phys. 73 (10), 106501–106588. doi:10.1088/0034-4885/73/10/106501.

McLauchlan, JamesIvey, 1931. The Humphrey pump and the installation of two sixty-six inch units at Cobdogla, river Murray. Trans. inst. 12, 413–426.

Morteza, Gharib, Edmond, Rambod, Karim, Shariff, 1998. A universal time scale for vortex ring formation. J. Fluid Mech. 360, 121–140. doi:10.1017/S0022112097008410.

Popov, O.E., Kogarko, S.M., 1976. One special feature of an underwater explosion of gas mixtures. Combustion, explosion and shock waves 12 (4), 554–558. doi:10.1007/BF00741151.

Rayleigh, O.M., 1917. On the pressure developed in a liquid during the collapse of a spherical cavity. Phyl. Mag. 34 (200), 94–98. doi:10.1080/14786440808635681.

Saurer, H. and Victora, H. Hydrojet engine for marine and submarine propulsion, U.S. Patent 3024598, March 13, 1952.

Schlichting, H., Gersten, K., 2000. Boundary-Layer Theory. Springer-Verlag, Berlin Heidelberg, p. 800.

Shah, Y.T., Pandit, A.B., Moholkar, V.S., 1999. Cavitation Reaction Engineering. Springer, US doi:10.1007/978-1-4615-4787-7.

Teslenko, V.S., Drozhzhin, A.P., Medvedev, R.N., 2014. Pulsation of cavitating vortex rings in water. Tech. Phys. Lett. 40 (11), 1021–1023. doi:10.1134/S1063785014110297.

Teslenko, V.S., Drozhzhin, A.P., Medvedev, R.N., Batraev, I.S., 2014. In-water gas combustion in linear and annular gas bubble. Thermophys. Aeromech. 21 (4), 479–488. doi:10.1134/S0869864314040088.

Teslenko, V.S., Drozhzhin, A.P., Medvedev, R.N., Batraev, I.S., October 16-19, 2014. Ignition of combustible gases in water. In: Springer Proceedings in Energy: 2nd International Congress on Energy Efficiency and Energy Related Materials, pp. 187–193. doi:10.1007/978-3-319-16901-9_23.

Teslenko, V.S., Manzhalei, V.I., Medvedev, R.N., Drozhzhin, A.P., 2010. Burning of hydrocarbon fuels directly in a water-based heat carrier. Combustion, Explosion, and Shock Waves 46 (4), 486–489. doi:10.1007/s10573-010-0064-y.

The Humphrey internal combustion pump, 1913. Surveyor 26 (9), 190–199. doi:10.1080/18324460.1913.10439088.

Zhdan, S.A., Mitrofanov, V.V., Sychev, A.I., 1994. Reactive impulse from the explosion of a gas mixture in a semiinfinite space. Combustion, Explosion, and Shock Waves 30, 657–663. doi:10.1007/BF00755833.